Saffman-Taylor fingers with adverse anisotropic surface tension

R. Combescot
Laboratoire de Physique Statistique de l'Ecole Normale Supérieure, 24 rue Lhomond, 75231 Paris Cedex 05, France
(Received 4 October 1993)

Viscous fingering in a linear channel is investigated analytically in the presence of adverse anisotropy, i.e., when the directions of easy growth are at angle π/m away from the direction of the cell axis because of the anisotropy of the surface tension. The study is made in the limit of small surface tension and for a finger width which is around one-half of the cell width. The analytical investigation reveals the existence of an exceptional solution for the Saffman-Taylor finger which does not belong to the standard manifold. The origin of this exceptional solution is clarified by a WKB analysis of the problem. This finger has a width which grows with velocity in contrast with the standard situation. This is in agreement with experimental observation for the stable fingers and for the averaged unstable ones.

PACS number(s): 68.10.−m, 47.20.Hw

I. INTRODUCTION

Saffman-Taylor fingering [1] is a most fascinating example of pattern selection. Indeed it is very accessible experimentally, and the theoretical situation does not look complicated once it is realized that surface tension is responsible for the selection [2]. Yet despite the apparent simplicity of the basic situation, Saffman-Taylor fingers provide a very rich physical situation because almost any small modification of this basic system seems to lead to new features in the selection process. More specifically Saffman and Taylor explored the case of a linear Hele-Shaw cell and found that, for large velocity, the finger width λ relative to the cell width goes to the limiting value $\lambda=\frac{1}{2}$. This limiting case seems actually fairly unstable since it is drastically modified under various small perturbations. For example, a small object [3] placed in front of the finger produces a narrow finger with λ much less than $\frac{1}{2}$. Similarly the replacement of the linear cell by a divergent sector [4] leads to a strong modification of the spectrum for the allowed finger width [5]. Finally Dorsey and Martin [6] showed that, in a linear cell, an anisotropy in the surface tension produced a finger width going to zero for large velocities. This anisotropy in the surface tension is reminescent of the physical situation found in solidification problems. Experimentally it is realized in a Hele-Shaw cell by engraving the plates for example.

In the present paper we are interested in a physical situation which is quite similar to the one considered by Dorsey and Martin. Indeed in their case the anisotropy of the surface tension was such that the surface tension is minimal at the tip of the finger. Precisely they investigated a surface tension $T(\theta)$ given by $T(\theta)=T[1-2\delta\cos(m\theta)]$ with θ being the angle between the normal $\mathbf{n}$ to the interface and the cell axis, and δ a positive constant. A surface tension minimal at the tip of the finger leads to a small radius of curvature at this tip, and one can guess intuitively that this produces narrow fingers as proved indeed by Dorsey and Martin. Here we are interested in the case of "negative" or "adverse" anisotropy where the modulation of the surface tension is of the opposite sign and gives a surface tension maximal at the tip of the finger: $T(\theta)=T[1+2\delta\cos(m\theta)]$ and δ still a positive constant. In this case the radius of curvature at the tip of the finger will be larger than in the standard case and one expects a fat finger which moves less rapidly than the standard one. Our motivation for studying this case is the experiment performed in this geometry which gives results [7,8] markedly different from the ones obtained for positive anisotropy, and very surprising by themselves. Indeed when the velocity of the finger gets larger, its width increases toward the full cell width whereas one would expect the finger to have a decreasing width, because a narrow finger can move faster than a wide one as it has less viscous fluid to displace. This result is in sharp contrast with the previously investigated cases where, as one might expect, the width of the average finger always decreases with the finger velocity.

There is, however, some qualitative difference between the experimental situations for positive and for negative anisotropy. In the range of large velocities which will be of interest for us, the finger becomes unstable and one obtains a fractal structure [9]. Previous experimental studies of these kinds of situations have shown a quite remarkable and surprising result both for the isotropic [10] and the anisotropic cases [7]: when one performs a proper average of different realizations of fractal growth, the result has the same shape and follows the same selection rules as the corresponding stable finger. Though there has been some progress in making sense of this result by the use of a modified mean field theory [11], it is not fully understood. Nevertheless we will heavily rely on it in order to relate our theoretical analysis to experiment since we will *assume* that the selection of the averaged unstable finger can be obtained from the selection of the stable one for the same value of the velocity. The agreement we find with experiment [8] is another piece of evidence which tends to show that this hypothesis is correct, but clearly a full theoretical justification would be highly desirable.

In this paper we will show that, in the presence of negative anisotropy, the spectrum for the selected values of the stable finger width contains, roughly speaking, a part

which is merely the spectrum of the standard finger (i.e., without anisotropy) slightly shifted toward larger width by the effect of the negative anisotropy, as we could expect intuitively from the argument given above. However, we will see that, quite unexpectedly, there appears also a branch which is an exceptional solution of the equations. More precisely this branch mixes slightly with the standard spectrum to produce the global spectrum that we actually obtain. Now the surprising observation is that the experimental result follows closely the exceptional branch. This provides naturally a nice and simple explanation for the experimental data. But we stress that we do not know why this rather peculiar branch is selected rather than, for example, the branch with lower finger width. Anyhow the existence of the exceptional branch is of general interest because we will see that its appearance is rather generic and is not linked to a very specific feature of the present problem. Therefore, although it is the first time to our knowledge that such an exceptional solution arises in a selection problem the possible existence of such a branch should be kept in mind when other shape selection problems are investigated. A short account of this work has already been published [8] together with the experiment and the results of a numerical simulation.

II. SELECTION FOR SMALL SURFACE TENSION

We start with the standard boundary condition due to surface tension, namely, the Laplace equation $\phi-\phi_0=b^2T(\theta)/12\mu R$, where b is the cell thickness, μ the viscosity of the viscous fluid, and R the radius of curvature of the interface. As usual we take the half width of the cell as unit length. The two-dimensional velocity field $\mathbf{u}$ (u_x,u_y) in this viscous fluid is related to the pressure p by Darcy's law $\mathbf{u}=-(b^2/12\mu)\nabla p$, which gives $\phi=-pb^2/12\mu$ for the velocity potential ϕ. In Laplace equation ϕ_0 corresponds to the pressure inside the finger. As we have indicated in the Introduction we take for the surface tension $T(\theta)=T[1+2\delta\cos(m\theta)]$, which amounts to retain the dominant Fourier component in $T(\theta)$. For the experiment that we consider $m=4$ should give a fair representation of the surface tension.

It is convenient for our purpose to rewrite the above boundary condition [12] in a somewhat different way. One takes the derivative of this relation with respect to arclength along the finger and combines it with the relation between finger velocity U and the fluid velocity: $\mathbf{n}\cdot\mathbf{u}=U\cos\theta$. If we take the fluid velocity at infinity equal to unity we have $\lambda U=1$. One obtains in this way the following differential equation along the finger [12]:

$$\varepsilon\frac{d}{dz}\left[[1+\delta(f^m+f^{-m})]\frac{df}{dz}\right]+\frac{1}{f^2}=2\lambda u-1\ , \qquad (1)$$

where $\varepsilon=b^2T/6\mu U$ and $f=e^{i\theta}$; $u=u_x-iu_y$ is the complex fluid velocity and $z=x+iy$ the complex position.

In order to perform an analytical study of the problem we will restrict ourselves to the regime of small surface tension T, or equivalently of large finger velocity U, which corresponds to small ε. This allows us to make use of a technique already employed [13] for standard Saffman-Taylor fingers where a singular perturbation analysis of the nonlinear differential equation (1) can be done in this limit. The selection is obtained by requiring that no transcendental divergent term is produced by the first term of Eq. (1), which acts as a singular perturbation for small surface tension.

We find the selection condition by continuing analytically Eq. (1) out of the finger into the viscous fluid. For small surface tension T, we can approximate u by its $T=0$ value, namely [1],

$$\frac{1}{u}\equiv\frac{dz}{dw}=\lambda+(1-\lambda)\tanh(\pi w/2)\ , \qquad (2)$$

where $w=\phi+i\psi$ is the complex velocity potential. The possible transcendental corrections to the $T=0$ solution are generated by the singularities of f, where the first term of Eq. (1) is no longer small. To lowest order in T, these are the singularities of the $T=0$ solution $f_0=(2\lambda u-1)^{-1/2}$ which diverges for $u=1/2\lambda$. For analytical convenience we restrict our study to finger widths λ in the vicinity of $\lambda\approx\frac{1}{2}$, because in this case $u\approx1$ and the singularities correspond to large w and z and we obtain simple analytical expressions. But our study could be extended in principle to other values of λ at the price of more numerical work.

In this regime of large w, we have $u\approx1+2(1-\lambda)e^{-\pi w}$. On the other hand, f^{-m} is negligible compared to f^m near the singularities of f. Taking $x=e^{-\pi w/2}\approx e^{-\pi z/2}$ as new variable we obtain

$$\varepsilon\left[\frac{\pi}{2}\right]^2 x\frac{d}{dx}\left[(1+\delta f^m)x\frac{df}{dx}\right]+\frac{1}{f^2}=2\lambda-1+x^2\ . \qquad (3)$$

This is just what is found in the isotropic case, except for the δf^m term due to anisotropy.

As usual we rescale this equation, by $f=[\varepsilon(\pi/2)^2]^{-1/3}F$ and $x=[\varepsilon(\pi/2)^2]^{1/3}X$, into

$$X\frac{d}{dX}\left[(1+DF^m)X\frac{dF}{dX}\right]+\frac{1}{F^2}=C+X^2\ , \qquad (4)$$

where C is a rescaled finger width and D a rescaled anisotropy

$$C=\frac{2\lambda-1}{[\varepsilon(\pi/2)^2]^{2/3}}\ ,\quad D=\frac{\delta}{[\varepsilon(\pi/2)^2]^{m/3}}\ . \qquad (5)$$

These relations provide scaling laws relating situations with different λ, ε, and δ, but same C and D. Naturally these scalings are valid only for small ε and $2\lambda-1$, as we mentioned above. For consistency we have also to assume a small δ in order to have a finite value for our parameter D.

The nonlinear differential equation Eq. (4) has to be solved with the boundary condition $F\approx1/y$ for large $|y|$ in the domain $|\arg y|\le\pi/2$ since we require that no transcendental divergent term is produced on the finger. For $D=0$ we have the standard Saffman-Taylor finger and, with these boundary conditions, there are solutions of Eq. (4) when the "nonlinear eigenvalue" C takes a discrete set of values C_n, well approximated by the result of a WKB analysis [13], namely, $C_n=2^{2/3}(n+\frac{4}{7})^{4/3}$ and

$n=0,1,\ldots$. These correspond to the well known branches of the finger width spectrum, all starting from $\lambda=\frac{1}{2}$ when the surface tension goes to zero.

In the presence of anisotropy $D\neq 0$, Eq. (4) can be solved numerically. This is done conveniently by taking $\ln x$ as a variable and [6] following for large $|x|$ the Stokes line $\arg x=\pi/3$, as an integration path, while turning toward the real axis when $|x|\sim 1$. By requiring that F is real on the real axis [13], one ensures that $F(y^*)=F^*(y)$ and that $F(y)$ behaves as $1/y$ for large $|y|$ and $-\pi/2\leq \arg y<0$. As a function of D the possible values of C do obviously change. We find naturally several branches, each one going to the corresponding C_n for $D=0$. The result for the lower branches of $C(D)$ is displayed on Fig. 1 for $m=4$. As noted in [8], our result agrees quite well for the three lowest branches with the direct numerical calculation on the finger in the regime of "large" surface tension. This can be seen in Fig. 2 of Ref. [8]. This is rather surprising since $2\lambda-1$ is not small at all where this agreement occurs, but such a surprisingly good agreement has also been found in the sector geometry [5]. At the very least this shows that our assumption of small $2\lambda-1$ is not a severe restriction.

On the other hand [8], there is a qualitative disagreement for the higher branches. Indeed the direct calculation on the finger displays the merging phenomenon of neighboring branches already found for the Saffman-Taylor finger in the sector geometry [5]. Instead the solution of Eq. (4) gives a kind of "anticrossing" between branches as can be seen from Fig. 1. One can also describe qualitatively Fig. 1 by saying that, for large D, the $n=0$ branch ends up on the natural continuation of the $n=1$ branch; similarly the $n=1$ branch switches to the $n=2$ branch and so on. The switch between branches occurs for $D\approx 2.5C^{8/7}$, as it is seen in Fig. 1 (this specific relation will be justified later on).

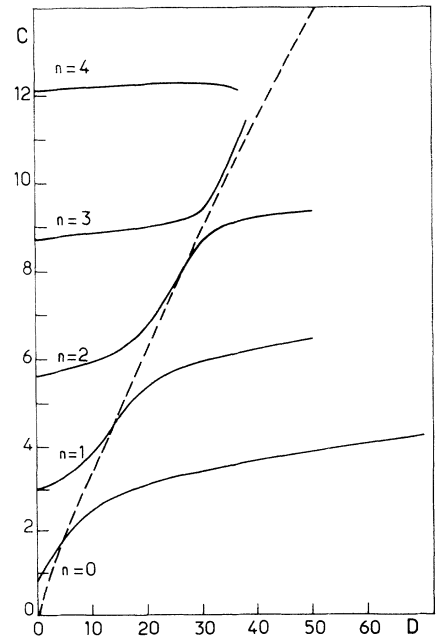

FIG. 1. Spectrum for the selected values of the rescaled finger width C as a function of the rescaled anisotropy D, for $m=4$. The branches corresponding to $n=0$, 1, 2, (partly) 3, and 4 are displayed. The dashed line corresponds to $D=2.5C^{8/7}$.

It can be seen from Fig. 2 of Ref. [8] that the anticrossing between branches and the merging in the direct calculation occur essentially at the same location, that is $2\lambda-1\approx 0.18^{7/8}/B^{1/2}$ with $B=\varepsilon/8$; this shows clearly that these behaviors are directly related. Actually, if the numerical calculation of Eq. (4) is not precise enough, one switches easily from anticrossing to merging. However, the precision of our numerics is good enough and we do not think that the origin of the discrepancy comes from numerical imprecision. We believe rather that anticrossing occurs for low anisotropy and surface tension, whereas branch merging happens for larger values. But one cannot exclude the possibility that the approximations leading to Eq. (4) are responsible for the switch from one behavior to the other. Anyway we note that the difference is irrelevant experimentally since the higher branches are not directly observable; only the lower one is relevant. The higher branches are observed indirectly (see above): only the *location* where merging or anticrossing occurs is important, the specific behavior cannot be seen.

III. THE LINEARIZED EQUATION

In order to understand the remarkable anticrossing behavior found in Fig. 1, we have performed an approximate analysis of Eq. (4). Although, it is valid in principle only for large values of C (that is small α, see below) this analysis has been quite successful even for the $n=0$ branch in the case of the standard Saffman-Taylor finger, in the linear [13] or the sector geometry [5]. In the present case similarly we will see that it leads to nearly exact results. For our purpose it is convenient to rescale Eq. (3) differently, or equivalently to rescale Eq. (4) by $F=C^{-1/2}G$ and $X=C^{1/2}Y$ into

$$\alpha Y\frac{d}{dY}\left[Y\frac{d}{dY}\left[G+\frac{a}{m+1}G^{m+1}\right]\right]+\frac{1}{G^2}=1+Y^2\,, \tag{6}$$

with $\alpha=C^{-3/2}$ and $a=DC^{-m/2}$. For small α, G will be very nearly equal to the zeroth order solution $G_0=(1+Y^2)^{-1/2}$ almost everywhere. If we set $G=G_0+h$, the small difference h will be solution of the equation obtained by linearizing Eq. (6). Introducing $H=h(1+aG_0^m)$, we have

$$Y\frac{d}{dY}\left[Y\frac{dH}{dY}\right]=\frac{2}{\alpha}H\frac{G_0^{-3}}{1+aG_0^m}+Y\frac{d}{dY}[Y^2(G_0^3+aG_0^{m+3})]\,. \tag{7}$$

When this equation is solved numerically, one finds for all branches results for $C(D)$ which are almost identical to those obtained from Eq. (4) and given on Fig. 1 for $m=4$. Therefore we can consider Eq. (7) as essentially equivalent to our original problem Eq. (6).

Now we can have more insight in the solutions of Eq. (7) in the following way. The solubility condition is that

H should be real on the real Y axis. In the vicinity of the origin $Y=0$, we can solve Eq. (7) to dominant order as

$$H\sim\exp\left[-\left[\frac{2}{\alpha(1+a)}\right]^{1/2}\ln Y\right] \tag{8}$$

[naturally H is no longer small in this region, but we are just solving the same equation (7) by looking at its analytical continuation]. Near the origin, on the positive imaginary Y axis, H has an argument $\varphi(\alpha,a)$ and from Eq. (8) the solubility condition reads

$$\varphi(\alpha,a)=n\pi-\frac{\pi}{2}\left[\frac{2}{\alpha(1+a)}\right]^{1/2} \tag{9}$$

or

$$C^{2/3}=2(1+a)\left[n-\frac{\varphi(\alpha,a)}{\pi}\right]^2, \tag{10}$$

which is the same as for the standard Saffman-Taylor finger [13], except for the factor $1+a$ and the fact that φ/π is no longer equal to $-\frac{4}{7}$. We have therefore the same branch structure as for the standard finger.

In order to find $\varphi(\alpha,a)$, we consider what happens on the positive imaginary axis for $0<|Y|<1$. We consider first the regime of small α. In this case the right hand side of Eq. (7) is dominated by its first term and the argument of H stays constant since G_0 is real on this interval. H is approximately given by the WKB expression

$$H\sim\left[\frac{G_0^{-3}}{1+aG_0^m}\right]^{-1/4}\times\exp\left[-\left[\frac{2}{\alpha}\right]^{1/2}\int^Y\frac{dY}{Y}\left[\frac{G_0^{-3}}{1+aG_0^m}\right]^{1/2}\right], \tag{11}$$

which matches Eq. (8) in the vicinity of $Y=0$. This description does not hold anymore in the vicinity of the turning point $Y=i$ where G_0 diverges: the first term of the right hand side of Eq. (7) vanishes while the second one diverges and the argument of H is no longer constant. Therefore we have to solve Eq. (7) in the vicinity of $Y=i$ and $\varphi(\alpha,a)$ is the limiting value of the argument of H far away from $Y=i$.

In the vicinity of $Y=i$, we have $G_0^{-2}\approx 2i(Y-i)$. We can then simplify Eq. (7) by a change of variable and a rescaling. Setting $Y=i[1-Z(\alpha^2/8)^{1/7}]$ and $H=(4\alpha)^{-1/7}g$, we obtain in the limit of small α

$$\frac{d^2g}{dZ^2}=2g\frac{Z^{(m+3)/2}}{Z^{m/2}+p}-\tfrac{3}{4}Z^{-5/2}-\frac{3+m}{4}pZ^{-(m+5)/2}, \tag{12}$$

where we have set $p=a(4\alpha)^{-m/7}$. This equation must be solved with the conditions that, for $|Z|\to\infty$, g vanishes in the Stokes sector $2\pi/7<\arg Z<6\pi/7$ and $6\pi/7<\arg Z<10\pi/7$. This is just the translation [13] of the conditions imposed on Eq. (4) or (7). However, g diverges in general for $\arg Z=0$ and large Z corresponding to the behavior given by Eq. (11).

We see that, in this limit of small α, $\varphi(\alpha,a)$ depends actually on the single parameter

$$p=\frac{a}{(4\alpha)^{m/7}}=\frac{D}{(2C)^{2m/7}}=\frac{\delta}{[\pi^2\varepsilon(2\lambda-1)^2]^{m/7}}. \tag{13}$$

We can check this result by calculating $\varphi(\alpha,a)$ from our results Fig. 1 through Eq. (9) and plotting the results in terms of p. If φ depends on this single parameter, the results for the various branches should fall on top of each other to give a single curve. This is done in Fig. 2 for $m=4$ and the branches $n=0,1,2,3$. We do not find a single curve, but this is not so surprising since we are not in the limit of small α for these low order branches. On the other hand, the curves seem to converge toward a jump of $-\pi$ for φ at $p\approx 1.1$. This is the translation of the switch between branches on Fig. 1 discussed previously. Indeed a change of φ by $-\pi$ transforms effectively the n branch into the $n+1$ branch. And $p\approx 1.1$ corresponds to the location $D\approx 2.5C^{8/7}$ of the anticrossing, which we have seen above.

There is now a simple explanation for the jump of φ by $-\pi$ that we have just found. Indeed in the vicinity of $Y=i$, Eq. (11) reduces to

$$g\approx\gamma\left[\frac{Z^{(m+3)/2}}{Z^{m/2}+p}\right]^{-1/4}\times\exp\left[\sqrt{2}\int^Z dZ\frac{Z^{(3+m)/4)}}{(p+Z^{m/2})^{1/2}}\right]. \tag{14}$$

The complex prefactor γ depends on p. If it vanishes for some value of p, the image of γ in the complex plane goes through the origin and this produces a switch of $\pm\pi$ for the argument of γ. Now if $\gamma=0$ this means that the divergent term Eq. (11) is absent. Since it reduces to Eq. (8) in the vicinity of $Y=0$, we do not have this divergent behavior. Rather from Eq. (7), we have in this vicinity $H(Y)\sim O(Y^2)+O(Y^{[2/\alpha(1+a)]^{1/2}})$, which goes to zero for

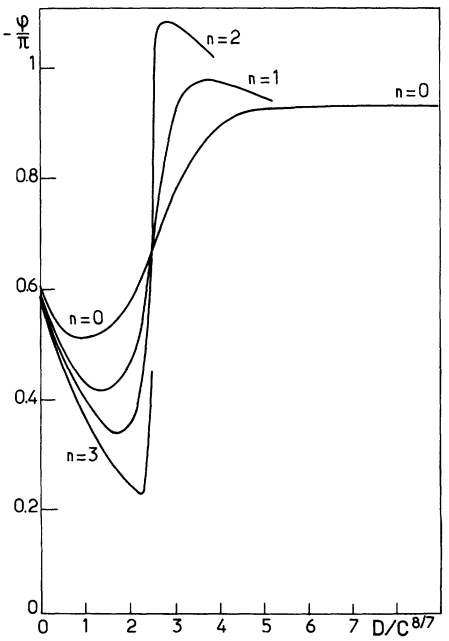

FIG. 2. Plot of $-\varphi(\alpha,a)/\pi$ as a function of $D/C^{8/7}=2^{8/7}p$, as obtained from Fig. 1 and Eq. (9), for the branches $n=0$, 1, 2, and 3.

$Y=0$. Since H must also go to zero for $Y\to\infty$, we have in this case a solution of Eq. (7) which is real on the real Y axis, and the solubility condition is satisfied [when we go outside the WKB regime, we have to generalize the condition $\gamma=0$ into $H(0)=0$]. Therefore we have for $\gamma=0$ a new solution for the Saffman-Taylor finger. But this is not a regular solution belonging to the family given by Eq. (10). This is rather a singular or exceptional solution. This provides our physical interpretation for the switch between branches observed in Fig. 1. It is produced by an exceptional solution given by $D\approx 2.5C^{8/7}$. When a regular branch meets this exceptional solution, it switches on it and then switches to the next regular branch encountered. This last switch may occur toward larger D, which produces the anticrossing behavior. It could also happen toward lower D which gives rise to the merging phenomenon (see below).

IV. THE EXCEPTIONAL SOLUTION

We will now go in more detail into the calculation of $\gamma(\alpha,a)$. We will see that, although the basic physical picture given above is correct, the actual situation is slightly more complicated. When we have an exceptional solution, Eq. (12) has a solution which goes to zero, for $|Z|\to\infty$, in the three Stokes sectors $-2\pi/7<\arg Z<2\pi/7$, $2\pi/7<\arg Z<6\pi/7$, and $6\pi/7<\arg Z<10\pi/7$. This is quite analogous to our original problem Eq. (7) except that presently we have Stokes sectors with an angle $4\pi/7$ instead of $4\pi/3$. In order to complete the analogy, we turn our reference axis by an angle $4\pi/7$, by setting $Z=e^{4i\pi/7}\zeta$ and $g=\tilde{g}e^{-2i\pi/7}$. When we substitute into Eq. (12), we obtain the same Eq. (12) except that Z and g are replaced respectively by ζ and $\tilde{g}$, and p is replaced by $\tilde{p}=pe^{-2i\pi m/7}$. Now we want a solution which goes to zero at infinity for the three sectors in $-6\pi/7<\arg\zeta<6\pi/7$. As for Eq. (4) or (7) this is obtained if the solution which goes to zero in $2\pi/7<\arg\zeta<6\pi/7$ and $-2\pi/7<\arg\zeta<2\pi/7$ for $|\zeta|\to\infty$ is real on the real ζ axis. Clearly this will be possible for some discrete values of $\tilde{p}$ if $\tilde{p}$ is real, in complete analogy with Eq. (7). And indeed one finds numerically such a solution for $\tilde{p}\approx -0.88$ (others are found for $\tilde{p}\approx -2.9,-5.26,\ldots$). However, this corresponds to a real positive value $p\approx 0.88$ only for $m=3.5$, not $m=4$. The p value is also slightly different from the value 1.1 found above. Therefore we do find an exceptional solution, but it is slightly away from what we expected. We note that it is clear from the start that we have to vary both p and m to find generically an exceptional solution. Indeed if we vary only p, γ will wander in the complex plane with no reason to go through the origin. This is only by varying also m that γ can become zero generically.

Therefore in order to understand what happens for $m=4$, we are led to consider other values of m. The results for the finger width spectrum C as a function of anisotropy D is displayed on Fig. 3 for $m=3.5$. We see on Fig. 3 that, when we lower m starting from $m=4$, the branches get increasingly well separated with the anticrossing structure fading away rapidly and being already basically absent for $m=3.5$ (however, the switch phenomenon from one branch to the next one is still clearly visible). For $m=3$ and 2 (not shown) the branches rise even more rapidly as a function of D, and they look unrelated. Although it is not of direct interest for our problem, we also show on Fig. 4 the results for $m=4.5$ because, instead of anticrossing, they display the phenomenon of branch merging between the branches $n=0$ and 1. As a result branch $n=2$ switches to branch $n=1$, similarly $n=3$ switches to $n=2$, and so on (the same qualitative behavior is found for $m=5$ and 7, but with the branches being well separated). Actually we believe that, for $m=4$, such a branch merging occurs be-

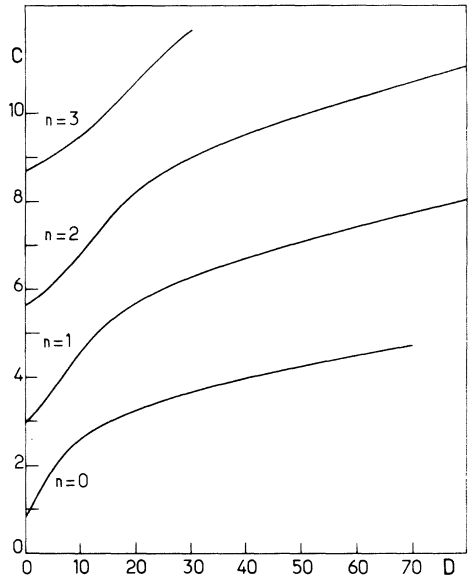

FIG. 3. Same as Fig. 1 for $m=3.5$.

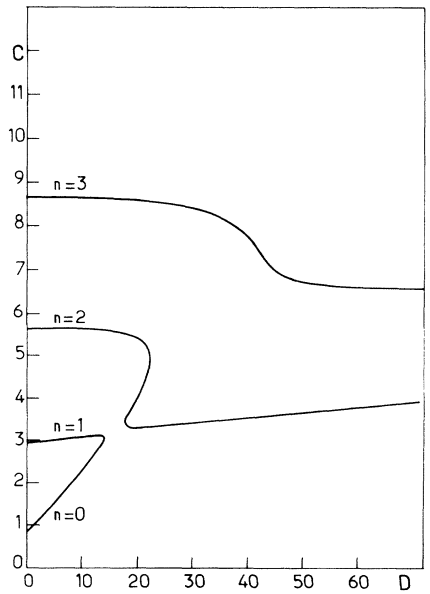

FIG. 4. Same as Fig. 1 for $m=4.5$.

tween the low D parts of the $n=3$ and 4 branches, but our numerical precision is not good enough to be sure of it. We note that the continuous evolution of the spectrum when m is changed is clearly seen from Figs. 1, 3, and 4.

We consider now the behavior of φ defined by Eq. (9). The results for $m=3.5$ are shown on Fig. 5. This value $m=3.5$ found above corresponds actually to a qualitative change in the behavior of φ as we will see. Let us first consider the case $m=2$ which is simple. Indeed when $\varphi(p)$ is calculated numerically directly from Eq. (12), one finds for $m=2$ that $-\varphi(p)/\pi$ rises regularly from its $p=0$ value [13] of $\frac{4}{7}$. It goes for large p to an asymptotic limit φ_∞, which can be obtained analytically as $-\varphi_\infty/\pi=(2m+4)/(m+7)$ [this is done from a symmetry argument on the WKB solution of Eq. (12), or by a Borel resummation as in [13]). Moreover the resulting values of φ are in very good agreement with the values of $\varphi(\alpha,a)$ obtained by direct integration of Eq. (4), making use of Eq. (9): in contrast to the case $m=4$, the various branches fall essentially on a single curve for $\varphi(p)$ which agrees itself with the result from Eq. (12). For $m=3$, the results are similar, except that $-\varphi(p)/\pi$ obtained from Eq. (12) has a small dip for $p\approx 0.4$ before rising and there is in this dip region a small discrepancy between this result from Eq. (12) and the direct integration of Eq. (4) (mostly for the branch $n=0$ which does not show any dip at all).

For $m=3.5$, the result from Eq. (12) is markedly different as it can be seen on Fig. 5: $-\varphi(p)/\pi$ decreases rapidly and linearly as p increases. Actually this result

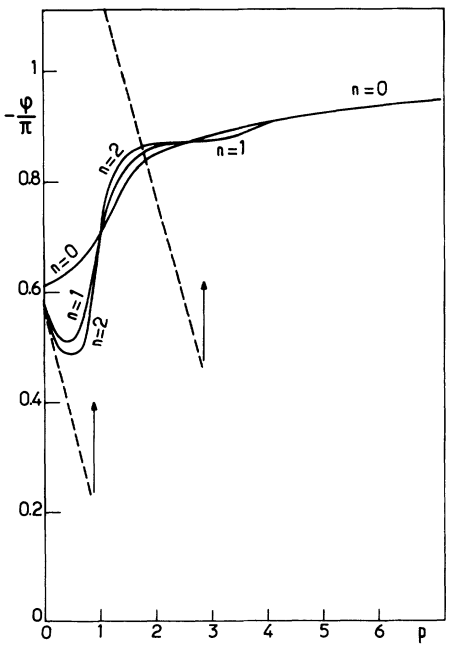

FIG. 5. Plot of $-\varphi(\alpha,a)/\pi$ as a function of p, as obtained from Fig. 3 and Eq. (9), for the branches $n=0$, 1, and 2. Branch $n=3$ is undistinguishable from branch $n=2$ on this graph. The dashed line indicates $-\varphi(p)/\pi$ obtained directly by integration of Eq. (12). The arrows indicate the jumps due to the exceptional solutions.

can be obtained analytically by a Borel resummation. One finds (in perfect agreement with numerics) $-\varphi(p)/\pi=\frac{4}{7}-2\sqrt{2}p/7$ (except for the additional jumps by 1 which occur for the exceptional solutions at $p\approx 0.88, 2.9, \ldots$ if we let $m-3.5=0_-$). On the other hand, the results from Eq. (4) are very similar to those of $m=3$: except for the $n=0$ branch at small p, they fall essentially on a single curve for $-\varphi/\pi$, which rises slowly for large p. For $m=4$, the result for $-\varphi(p)/\pi$ from Eq. (12) is similar to the one found for $m=3.5$. It agrees with the results from Eq. (4) only for small p.

This behavior can be understood qualitatively in the following way. One notices that Eq. (12) has a singular point for $Z_0=(-p)^{2/m}$, which is a branch point for the corresponding WKB solution Eq. (14) [one has to take the determination corresponding, in Eq. (14), to go around Z_0 on the large $|Z|$ side]. Now the solution of Eq. (12) must vanish for $|Z|\to\infty$ in the sectors $2\pi/7<\arg Z<6\pi/7$ and $6\pi/7<\arg Z<10\pi/7$. Numerically we enforce these conditions by starting on the Stokes line $\arg Z=6\pi/7$ for large $|Z|$, with g and dg/dZ equal to zero. We integrate then Eq. (12) through the sector $2\pi/7<\arg Z<6\pi/7$ to go on the real Z axis and find $\varphi(p)$. Depending on the value of m, Z_0 is or is not in the sector $0<\arg Z<6\pi/7$ relevant for our calculation. For $m=2$, Z_0 is on the real negative axis and the branch point is irrelevant for our calculation. This corresponds to the small rise of $-\varphi(p)/\pi$ from $\frac{4}{7}$ to $\frac{8}{9}$ when p goes from 0 to ∞.

For $m=3$ one has to realize that, because of the branch point, the lines where, in Eq. (14), the argument of $\int^Z dZ\, Z^{(3+m)/4}(p+Z^{m/2})^{-1/2}$ is constant are distorted and are no longer straight lines starting from $Z=0$ as in the case $p=0$, or $m=0$. This is also true for our Stokes lines where the above argument is $\pi/2$ or $3\pi/2$ (Stokes line $2\pi/7$ or $6\pi/7$). In particular the Stokes line $6\pi/7$ starts actually with $\arg Z=6\pi/(7+m)$ from $Z=0$. For $m=3$, this is $3\pi/5$, which is less than $\arg Z_0=2\pi/m=2\pi/3$. Therefore the branch point Z_0 is again not in the Stokes region relevant to our calculation (although it is close). This allows one to understand why $\varphi(p)$ for $m=3$ is similar to $\varphi(p)$ for $m=2$.

Now for $m=3.5$, the Stokes line which has $\arg Z=6\pi/7$ for large $|Z|$ starts from $Z=0$ with $\arg Z=4\pi/7=\arg Z_0$. Therefore the branch point Z_0 is no longer in an irrelevant Stokes region (actually the $6\pi/7$ Stokes line wraps completely around the cut which goes from 0 to Z_0 and leaves again $Z=0$ with $\arg Z=20\pi/21$ and then goes to $\arg Z=6\pi/7$ for large Z). This explains why we find a marked change of behavior for $m=3.5$ (we note, however, that the jumps by 1 occurring at the exceptional solutions make $-\varphi(p)/\pi$ effectively rise as a function of p, just as for $m<3.5$; this provides a kind of continuous transition). For $m=4$, the cut $[0,Z_0]$ is again in the relevant Stokes region and $-\varphi(p)/\pi$ decreases again rapidly as a function of p. One can actually understand this behavior semiquantitatively by saying that, in addition to the standard contribution to φ found for $m<3.5$, which has a weak p dependence, there is an additional contribution to φ from the integral around the cut in Eq. (14). This argu-

ment gives a result which is in good agreement with the numerical integration of Eq. (12).

To summarize this discussion, when the branch point Z_0 is in an irrelevant region, as it happens for $m<3.5$, $-\varphi(p)/\pi$ has a gentle rise. When the branch point is relevant, which happens for $m\geq 3.5$, $-\varphi(p)/\pi$ drops rapidly as a function of p. This gives us a simple understanding of $\varphi(p)$ as it comes out from Eq. (12). But this does not explain the discrepancy for $m=3.5$ and 4 between these results and the direct calculation from Eq. (4). This discrepancy is at first surprising since for $m=3.5$, as we have mentioned, the results of the various branches for $\varphi(p)$ fall essentially on a single curve, giving the impression that a WKB limit is already reached.

This can be understood as follows. One can check that the condition for the WKB approximation is satisfied as soon as C is large which explains why it works already for the branches that we have considered. On the other hand, we have seen that the branch point Z_0 plays an essential role in our results for the solution of Eq. (12) (our integration path for example has to satisfy $|Z|>|Z_0|$). However, when we have obtained Eq. (12), we have neglected $(\alpha^2/8)^{1/7}Z$ with respect to 1 because α was assumed to be small. When this is not done, one can still evaluate (by taking G_0 as a variable) the argument of $\int_1^{Y_0}(dY/Y)G_0^{-3/2}(1+aG_0^m)^{-1/2}$, which comes in Eq. (11), with Y_0 being the branch point which satisfies $1+aG_0^m=0$. One can then easily see that this argument is larger than the corresponding value $(7+m)/2m$ obtained in the limit of small α(essentially when we write $Y=i[1-Z(\alpha^2/8)^{1/7}]$ instead of $Y=i$, we effectively increase the considered argument). This effect is larger for larger p and lower branches [the relevant parameter is $(\alpha^2/8)^{1/7}|Z_0|\sim a^{2/m}$].

This means that for large p and low branches, the branch point is pushed in the Stokes region where it is ineffective. This is as if we had effectively lowered the value of m. This explains why the results from Eq. (4) for $m=3.5$ and low branches are similar to those of Eq. (12) for $m=3$ (and even $m=2$ for the branch $n=0$). Similarly when we go to lower branches for $m=4$ in Fig. 2, we shift effectively toward the behavior corresponding to lower m [for example, the branch $n=0$ in Fig. 2 is very similar to what one obtains from Eq. (12) for $m=3$]. If we were to go to higher branches we would progressively go to the results for $\varphi(p)$ obtained from Eq. (12) for $m=4$. But since $a^{2/m}=0.3$ implies $C\approx 40$ for $p=1$, this would require us to go to much higher branches. This would be quite difficult numerically. On the other hand, we can merely check what we have just said by setting $Y=i[1-Z(\alpha^2/8)^{1/7}]$ and $H=(4\alpha)^{-1/7}g$ in Eq. (7) without assuming further that α is small as in Eq. (12). When the corresponding equation is solved for $\varphi(a,\alpha)$, one obtains results in perfect agreement with our arguments.

In summary we have been able to understand the origin of the peculiar anticrossing behavior found in our spectrum. It is due to the existence of an exceptional solution for the Saffman-Taylor finger, different from the ones corresponding to the ordinary branches of the spectrum. This exceptional solution is expected to occur for $m=3.5$ for high values of C. But for lower values of C one finds an actual behavior which corresponds to a value of m lower than the nominal one. This explains why the anticrossing behavior occurs for $m=4$ for the lower branches instead of $m=3.5$.

ACKNOWLEDGMENTS

We are grateful to V. Hakim for information on Ref. [6] and discussions in the early part of this work. We have benefited from numerous discussions with M. Ben Amar and Y. Couder when trying to understand what are the physical effects of adverse anisotropy. The Laboratoire de Physique Statistique is "associé au CNRS et aux Universités Paris 6 et Paris 7."

[1] P. G. Saffman and G. I. Taylor, Proc. R. Soc. London, Ser. A **245**, 312 (1958).

[2] J. M. Vanden-Broek, Phys. Fluids **26**, 2033 (1983); B. I. Shraiman, Phys. Rev. Lett. **56**, 2028 (1986); D. C. Hong and J. S. Langer, *ibid.* **56**, 2032 (1986); R. Combescot, T. Dombre, V. Hakim, Y. Pomeau, and A. Pumir, *ibid.* **56**, 2036 (1986); S. Tanveer, Phys. Fluid **30**, 1589 (1987).

[3] Y. Couder, N. Gerard, and M. Rabaud, Phys. Rev. A **34**, 5175 (1986).

[4] H. Thomé, M. Rabaud, V. Hakim, and Y. Couder, Phys. Fluids A **1**, 224 (1989).

[5] M. Ben Amar, Phys. Rev. A **44**, 3673 (1991); R. Combescot and M. Ben Amar, Phys. Rev. Lett. **67**, 453 (1991).

[6] A. T. Dorsey and O. Martin, Phys. Rev. A **35**, 3989 (1987).

[7] Y. Couder, F. Argoul, A. Arnéodo, J. Maurer, and M. Rabaud, Phys. Rev. A **42**, 3499 (1990).

[8] M. Ben Amar, R. Combescot, and Y. Couder, Phys. Rev. Lett. **70**, 3047 (1993).

[9] Y. Couder, in *Chaos, Order and Patterns*, edited by R. Artuso, P. Cvitanovic, and G. Cassati (Plenum, New York, 1991), pp. 203–227.

[10] A. Arneodo, Y. Couder, G. Grasseau, V. Hakim, and M. Rabaud, Phys. Rev. Lett. **63**, 984 (1989).

[11] E. Brener, H. Levine, and Yuhai Tu, Phys. Rev. Lett. **66**, 1978 (1991).

[12] R. Combescot and T. Dombre, Phys. Rev. A **38**, 2573 (1988).

[13] R. Combescot, T. Dombre, V. Hakim, Y. Pomeau, and A. Pumir, Phys. Rev. A **56**, 1270 (1988).